Bone Turnover Mediates Preferential Localization of Prostate Cancer in the Skeleton

Article *in* Endocrinology · May 2005

DOI: 10.1210/en.2004-1211 · Source: PubMed

0013-7227/05/$15.00/0
Printed in U.S.A.

Endocrinology 146(4):1727–1736

doi: 10.1210/en.2004-1211

Bone Turnover Mediates Preferential Localization of Prostate Cancer in the Skeleton

Abraham Schneider, Linda M. Kalikin, Ana C. Mattos, Evan T. Keller, Matthew J. Allen, Kenneth J. Pienta, and Laurie K. McCauley

Department of Periodontics/Prevention/Geriatrics, School of Dentistry (A.S., A.C.M., L.K.M.), Departments of Urology (L.M.K., E.T.K., K.J.P.), Pathology (E.T.K., L.K.M.), and Internal Medicine (Division of Hematology/Oncology), Medical School (K.J.P.), University of Michigan, Ann Arbor, Michigan 48109; and Department of Orthopedic Surgery (M.J.A.), State University of New York Upstate Medical University, Syracuse, New York 13210

Bone metastasis is a common untreatable complication associated with prostate cancer. Metastatic cells seed in skeletal sites under active turnover containing dense marrow cellularity. We hypothesized that differences in these skeletal-specific processes are among the critical factors that facilitate the preferential localization of metastatic prostate cancer in bone. To test this, athymic mice were administered PTH to induce bone turnover and increase marrow cellularity daily 1 wk before and after intracardiac inoculation of luciferase-tagged PC-3 cells. Tumor localization was monitored by bioluminescence imaging weekly for 5 wk. At the time of tumor inoculation, PTH-treated mice demonstrated significant increases in serum levels of bone turnover markers such as osteocalcin and tartrate-resistant acid phosphatase 5b and in the number of tartrate-resistant acid phosphatase-positive osteoclasts per millimeter of bone when compared with the other groups. Likewise, PTH treatment stimulated a qualitative increase in marrow cellular proliferation as determined by 5-bromo-2′-deoxyuridine immunostaining. Skeletal metastases formed in the hind limb and craniofacial regions of young mice with no difference between groups. In adult mice, however, bioluminescent signals in the hind limb and craniofacial regions were 3-fold higher in PTH-treated mice *vs.* controls. Fluorochrome labeling revealed increased bone formation activity in trabecular bone adjacent to tumors. When zoledronic acid, a nitrogen-containing bisphosphonate that inhibits osteoclast-mediated bone resorption, was administered concurrently with PTH, a significant reduction in the incidence of bone tumors was observed. Overall, these studies provide new evidence that skeletal sites rich in marrow cellularity under active turnover offer a more congenial microenvironment to facilitate cancer localization in the skeleton. (*Endocrinology* 146: 1727–1736, 2005)

PROSTATE CANCER CONTINUES to be a leading cause of cancer-related illness and the second most common cause of cancer-associated mortality, resulting in approximately 29,000 deaths per year in the United States (1, 2). One of the most debilitating and untreatable complications associated with prostate cancer is the development of bone metastases, which affects up to 90% of patients dying with advanced disease (3). Despite recent progress in prevention, diagnosis, and therapy, it remains unclear why this tumor demonstrates an organ-specific pattern of dissemination by preferentially colonizing the skeleton. Once localized in the bone microenvironment, the interaction of tumor cell-derived factors and bone cells results in the development of predominantly osteoblastic lesions likely generated by the dysregulation of the normal bone remodeling process. Whereas blastic lesions represent the most common osseous response to prostate cancer, in many instances the formation of blastic and lytic mixed lesions is also observed (4, 5).

According to the "seed and soil" hypothesis of cancer dissemination, the preferential ability of certain solid tumors to form distant metastases is closely dependent on a compatible microenvironment capable of supporting secondary tumor localization and growth (6). Within the skeleton, prostate cancer often spreads to the axial skeleton and long bone metaphyses, sites under active remodeling that contain increased marrow cellularity. These findings are supported by serial bone scanning, which confirms that metastases frequently localize to actively remodeled areas like the thoracolumbar spine, pelvis, ribs, and proximal femur (7). Thus, multiple bioactive factors derived from these osseous locations and resident cells within their bone marrow may play a major role in promoting tumor localization and subsequent growth (8, 9). Studies that have used bisphosphonates support the hypothesis that bone turnover contributes to tumor localization (10–12). However, these studies are not always in agreement (13), and bisphosphonates may have direct tumor effects that could be confounding. Furthermore, studies evaluating the impact of increasing bone turnover, as is typical from a calciotropic hormone such as PTH, are lacking.

Experimental murine models of skeletal metastasis have provided strong evidence for the seed and soil hypothesis (10, 14). However, conventional outcome analyses in these models have frequently relied on serial kills, meticulous microdissection to localize metastatic bone lesions, radiography, and histological examination. The advent of novel optical imaging technology to monitor tumor cells expressing bioluminescent reporter proteins has enormously improved

First Published Online January 6, 2005

Abbreviations: BLI, Bioluminescence imaging; BrdU, 5-bromo-2′-deoxyuridine; rh, recombinant human; TRAP, tartrate-resistant acid phosphatase; ZA, zoledronic acid.

***Endocrinology* is published monthly by The Endocrine Society (http://www.endo-society.org), the foremost professional society serving the endocrine community.**

the application of animal models in cancer research (15–17). Recently, we reported that young immunodeficient mice (average 7 wk old) developed significantly more bone metastases than older mice (average 1 yr old) after intracardiac inoculation of luciferase-tagged PC-3 human prostate cancer cells (PC-3^{Luc}) (18). Using weekly *in vivo* bioluminescence imaging (BLI) to monitor tumor localization and growth, we observed skeletal metastases developing progressively at the hind limb metaphyses and the craniofacial region as early as 1 wk after intracardiac injection. These results suggest that sites with active osseous turnover and higher cellular activity, as occur in young growing mice, may provide a more congenial microenvironment for successful prostate cancer skeletal seeding and growth.

Although the important role played by the bone marrow microenvironment in supporting prostate cancer growth in the skeleton has been extensively studied (4), validation of critical organ-specific factors that might contribute to the preferential localization of prostate cancer in bone is lacking. The purpose of the present investigation was to determine the impact of bone cellular activity and turnover on prostate cancer skeletal localization. Immunodeficient mice were administered recombinant human (rh)PTH [1–34] daily for 1 wk before and after intracardiac inoculation of PC-3^{Luc} cells. PTH was selected because of its well-established effects as a potent stimulator of bone turnover. In the skeleton, PTH is capable of stimulating both catabolic and anabolic actions, depending on the dose and mode of administration (19). Our results demonstrate that skeletal metastatic foci monitored for 5 wk by BLI were significantly increased in PTH-treated adult mice compared with saline-treated controls. Moreover, when zoledronic acid (ZA), a potent amino-bisphosphonate that inhibits osteoclastic activity (20), was administered to adult mice in conjunction with PTH, skeletal metastases were markedly reduced. These data provide evidence that bone turnover may serve as a unique organ-specific component that favors prostate cancer localization in the skeleton. Furthermore, these studies suggest that prostate cancer patients at risk of developing skeletal metastases might benefit from early monitoring of bone turnover markers, and if elevated, implement pharmacological preventive measures to limit bone remodeling.

Materials and Methods

Cells

PC-3, a spontaneously immortalized cell line derived from a human vertebral prostate cancer metastasis, was purchased from the American Type Culture Collection (Rockville, MD). A highly bioluminescent clone (PC-3^{Luc}) was developed after transfection with a luciferase-expressing pLazarus retroviral construct as previously described (21) except that Fugene 6 (Roche Applied Science, Indianapolis, IN) was used. PC-3^{Luc} cells were maintained at 37 C in phenol red-containing RPMI 1640 (Invitrogen Corp., Grand Island, NY) supplemented with 10% (vol/vol) fetal bovine serum (HyClone, Logan, UT), 100 U/ml penicillin, 100 μg/ml streptomycin, and 2 mM L-glutamine (Invitrogen Corp.) in a 5% CO_2 humidified chamber.

PC-3^{Luc} cell inoculation

Under anesthesia with 1.75% isofluorane/air, young (5–6 wk old) or adult (15 wk old) male athymic mice (Harlan Sprague Dawley, Houston, TX) were injected with PC-3^{Luc} cells [2×10^5 cells in 100 μl Dulbecco's PBS lacking Ca^{2+} and Mg^{2+} (Life Technologies, Inc., Grand Island, NY)] into the left ventricle according to the technique described by Guise *et al.* (14). All experimental animal procedures were performed in compliance of the institutional ethical requirements and approved by the University of Michigan Committee for the Use and Care of Animals. Intracardiac injections were performed 1 wk after daily sc administration of 0.9% sodium chloride (saline), rhPTH [1–34] (80 μg/kg; Bachem, Torrance, CA), or rhPTH [1–34] (80 μg/kg) in combination with ZA (3 μg/d; Novartis Pharma AG, Basel, Switzerland). These treatments continued for 1 wk after intracardiac inoculations. BLI was performed weekly for 5 wk after inoculation. A subset of animals from each group was killed after 1 wk of treatment to characterize changes occurring in bone turnover at the time of tumor cell inoculation. Before they were killed, the mice were anesthetized and terminal serum samples were collected by cardiac aspiration.

In vivo BLI

In vivo BLI was carried out at the University of Michigan Small Animal Imaging Resource facility (MSAIR; http://www.med.umich.edu/msair/) as previously described (16, 18). Briefly, imaging was performed under 1.75% isofluorane/air anesthesia on a cryogenically cooled IVIS system equipped with a 50-mm lens and coupled to a data-acquisition PC running LivingImage software (Xenogen Corp., Alameda, CA). Before imaging, mice were injected ip with 100 μl of 40 mg/ml luciferin dissolved in PBS. Ventral images were acquired 15 min after injection. Pseudo-color images of photon emissions were overlaid on grayscale images of mice to aid in determining signal spatial distribution. Photon quantifications were calculated within regions of interest. After the mice were killed, radiographs of hind limbs and mandibles were taken on a microradiography apparatus (model MX20; Faxitron XRay Corp., Buffalo Grove, IL).

Histology

BLI-positive hind limbs and mandibles from each group together with a similar number of negative BLI specimens as controls were dissected and fixed in 10% formalin for 24–48 h at 4 C. In the subset of adult mice killed after 1 wk of saline, PTH, or PTH/ZA treatment, tibiae were dissected and fixed following a similar protocol as described above. All specimens were decalcified in 10% EDTA (pH 7.4) for 10 d (femora/tibiae) or 21 d (mandibles) and embedded in paraffin, and 5-μm serial sections were prepared and then stained with hematoxylin/eosin. Tibial sections obtained from the subset of adult mice treated for only 1 wk were also used to characterize tartrate-resistant acid phosphatase (TRAP)-positive osteoclasts using a leukocyte acid phosphatase staining kit as previously described (22). In similar sections, cell proliferation was evaluated by 5-bromo-2′-deoxyuridine (BrdU) staining (Zymed, South San Francisco, CA) following the manufacturer's instructions. Dynamic bone histomorphometry was performed in fluorochrome-labeled femora dissected from PTH- or saline-treated adult mice killed at 5 wk after tumor cell intracardiac inoculation. Briefly, 100 μl of 15 μg/kg of calcein (Sigma, St. Louis, MO) dissolved in PBS containing 2% sodium bicarbonate was injected ip 10 d and 3 d before the mice were killed as described (23). The dissected bones were stored in 70% ethanol until further processing. Femora were embedded in methylmethacrylate as described by Erben (24). Serial step sections were carried out at 5 μm to approximately half way through the frontal plane of the bone, and series of 100 μm were collected every 50–100 μm. Quantification of fluorescent calcein-labeled bone surfaces per total area was carried out in the distal metaphyses of tumor- and non-tumor-containing femora by computer-assisted histomorphometry using Image Pro Plus 4.5 (Media Cybernetics, Silver Spring, MD) and SPOT RT 3.0 (Diagnostic Instruments, Sterling Heights, MI) software interfaced with a Nikon Eclipse E800 light/epifluorescent microscope (Nikon, Melville, NY).

Serum biochemistry

Changes in markers of bone turnover at the time of PC-3^{Luc} cell inoculation were determined by analyzing serum osteocalcin, a marker of bone formation, and serum TRAP 5b, a specific marker of osteoclastic bone resorption. Serum osteocalcin levels were determined by a RIA according to the manufacturer's protocol (Biomedical Technologies,

Stoughton, MA). Serum TRAP 5b levels were measured with the Mouse-TRAP assay per the manufacturer's instructions (IDS Inc., Fountain Hills, AZ).

Statistics

The data were analyzed using Student's *t* test with the Instat 2.1 biostatistics software (GraphPad Software, San Diego, CA). Data are presented as mean ± SEM.

Results

To determine the influence of increased bone turnover in prostate cancer skeletal localization, three independent studies were performed (Fig. 1). Initially, young male athymic mice were used to test the hypothesis that active bone turnover provides a more fertile microenvironment for prostate cancer localization to bone (Fig. 1A). Four-week-old mice were started on a daily regimen of sc administered rhPTH [1–34] (80 μg/kg) or saline for 1 wk before and after the intracardiac inoculation of PC-3^{Luc} cells. We selected PTH because of its well-studied effects as a stimulator of bone turnover. PTH is known for exerting dual actions in the skeleton; when administered continuously, PTH leads to a net bone loss, whereas an intermittent regimen results in an anabolic effect characterized by an increase in skeletal mass (25). At the dosing regimen used in our investigation, recent studies report that the osseous response to daily sc PTH treatment in murine and rodent model systems is associated with increases in femoral and tibial bone mass and markers of bone turnover, such as serum osteocalcin and bone extract alkaline phosphatase (markers of bone formation) as well as TRAP (marker of bone resorption) (26, 27). Therefore, we took advantage of these unique PTH-induced, skeletal-related properties to stimulate bone turnover in our experimental model.

One week after PC-3^{Luc} intracardiac inoculation, which coincided with the conclusion of pharmacological treatments, BLI was initiated and performed weekly for 5 wk to monitor the localization of luciferase-tagged tumor cells in the skeleton. In young mice, at 5 wk, PC-3^{Luc} cells were detected in areas such as the hind limb and craniofacial regions with no differences in the distribution of tumor foci between groups (Fig. 2, A and B, E and F). Skeletal BLI-positive signals were observed in 67% of mice from each group. Interestingly, positive craniofacial signals were present in all of these mice, whereas hind limb PC-3^{Luc} foci were only visualized in 50% of the mice from both groups. In some animals, BLI signals were detected as early as 1 wk after intracardiac injections, affecting one or both tibiae/femora and the craniofacial region.

Once in the bone microenvironment, human-derived PC-3 prostate cancer cells commonly stimulate the development of osteolytic metastatic lesions (18, 28). We verified the presence of these types of lesions and osteoclastic cells adjacent to PC-3^{Luc} tumor cells by radiographic and histological analyses, respectively. In the proximal tibia, lytic lesions were characterized by resorptive cavities containing multinucleated osteoclasts involving the metaphyseal region (Fig. 2, C and D). In the craniofacial region, tumor cells disseminated to areas affecting the periodontal ligament space of mandibular teeth. These lesions were characterized by the presence of active osteoclasts lining the endosteal surface of the alveolar bone (Fig. 2, H–J).

In the second part of the study, we used adult mice (15 wk

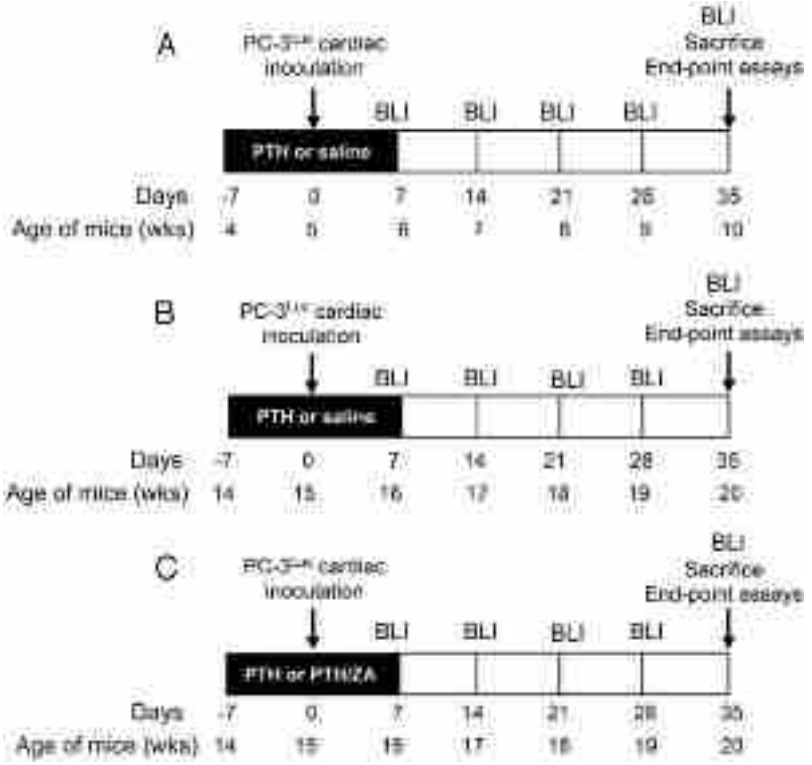

FIG. 1. Experimental protocol. Five-week-old (A; n = 6 mice per group) or 15-wk-old athymic male mice (B; n = 9 mice per group) were administered sc injections of rhPTH [1–34] (80 μg/kg) or saline daily for 7 d before and 7 d after the intracardiac inoculation of PC-3^{Luc} cells. At the conclusion of pharmacological treatment, BLI was initiated and conducted weekly for four more weeks to monitor PC-3^{Luc} localization. At d 35, animals were killed and end-point assays were performed as described in *Materials and Methods*. C, A similar approach as followed for panels A and B was used in 15-wk-old athymic male mice (n = 12–13 mice per group) that were treated with rhPTH [1–34] (80 μg/kg) with or without the simultaneous injection of ZA (3 μg/d). *Black boxes* illustrate pharmacological treatment period with either saline, PTH, or PTH/ZA.

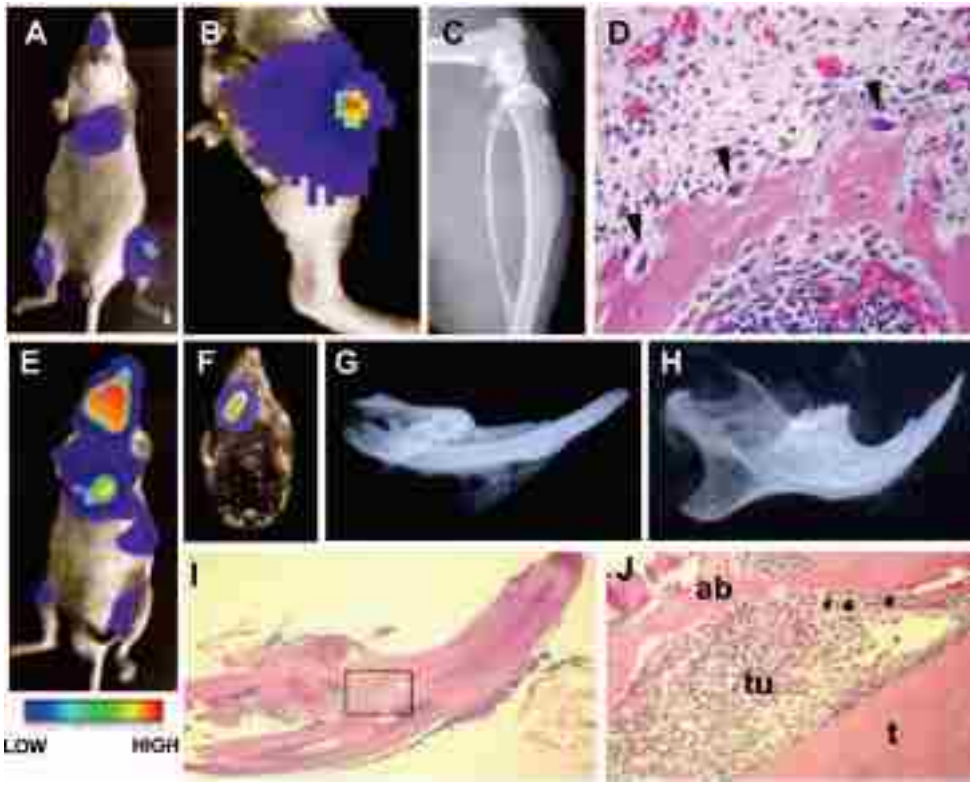

FIG. 2. PC-3^{Luc} cell localization in the hind limb and craniofacial regions in young mice. A, At 5 wk after the intracardiac inoculation of PC-3^{Luc} cells, positive BLI signals were observed in the hind limbs and craniofacial region in a representative saline-treated mouse. B, At the time of death, a positive BLI signal continued to be emitted and localized to the dissected left hind limb. A lesion in the proximal tibial metaphysis was confirmed by radiography (C) as a distinct radiolucent osteolytic lesion and histologically (D) by the presence of active, multinucleated osteoclastic cells inside resorptive lacunae (*arrowheads*) (×200). E, In a representative rhPTH [1–34]-treated mouse, an intense BLI signal was observed in the craniofacial region 5 wk after tumor inoculation. F, The BLI signal in the dissected head localized to the right hemimandible. This was associated with severe bone destruction as seen in the microradiograph (G) compared with the unaffected left hemimandible (H). I, PC-3^{Luc} cells invaded the periodontal ligament space adjacent to the right lower incisor (*box*, ×20). J, Higher magnification of box depicted in I demonstrates tumor cells (tu) localized between the tooth root surface (t) and the alveolar bone (ab). The endosteal surface of the alveolar bone is lined by several osteoclastic cells actively resorbing bone (*arrowheads*) (×100).

of age at the time of PC-3^{Luc} cell inoculation) because these mice have a lower incidence of skeletal localization compared with young mice (18). By using adult mice, we intended to rule out any inherent increase in bone cellular activity occurring in young mice as a consequence of their normal skeletal growth. After a similar experimental protocol (Fig. 1B), BLI demonstrated that adult mice treated with rhPTH [1–34] developed significantly more skeletal metastases in the hind limb and craniofacial regions at 5 wk after PC-3^{Luc} cell inoculation compared with saline-treated mice (Fig. 3). The mean number of BLI-positive total skeletal sites per mouse, which included both the hind limb and craniofacial regions, were 3-fold higher in rhPTH [1–34]-treated mice (1.67 ± 0.37) compared with saline controls (0.56 ± 0.18) (Fig. 3C). Interestingly, hind limb metastases were only observed in mice treated with rhPTH [1–34] (Fig. 3D), whereas in the craniofacial region both groups showed positive BLI signals. Although more mean positive signals per mouse were observed in the craniofacial region in the PTH group, differences with the saline-treated controls did not reach statistical significance (Fig. 3E).

To characterize the active, mineralizing osseous tissue present in tumor- and non-tumor-containing bones, the fluorochrome labeling agent calcein was injected into all mice 3 and 10 d before the mice were killed. We observed a significant increase in the percentage of calcein uptake at trabecular bone surfaces per total area in tumor-bearing rhPTH [1–34]-treated mice (4.58 ± 0.34) *vs.* the uptake in non-tumor-bearing mice treated with either rhPTH [1–34] or saline (2.87 ± 0.22) (Fig. 4, A–C). Although PC-3 cells are known for promoting predominantly osteolytic lesions, our results suggest that these cells are also capable of stimulating a local osteoblastic response in bony areas adjacent to the tumor lesion, possibly representing an attempt to repair lost bone (29). To our knowledge, this is the first report of increased bone formation activity in this widely used PC-3 prostate cancer cell model. This response could be associated with the activity of tumor-derived specific factors known to stimulate osteoblastic cells and promote bone formation (30). Furthermore, the marked increase in mineralizing bone surfaces observed only in the rhPTH [1–34]-treated mice bearing tumors and not in tumor-free animals from this same PTH-treated group supports the notion that this effect was dependent on the interactions between tumor cells and bone and independent of PTH administration. This is also consistent because the analysis was performed in femora dis-

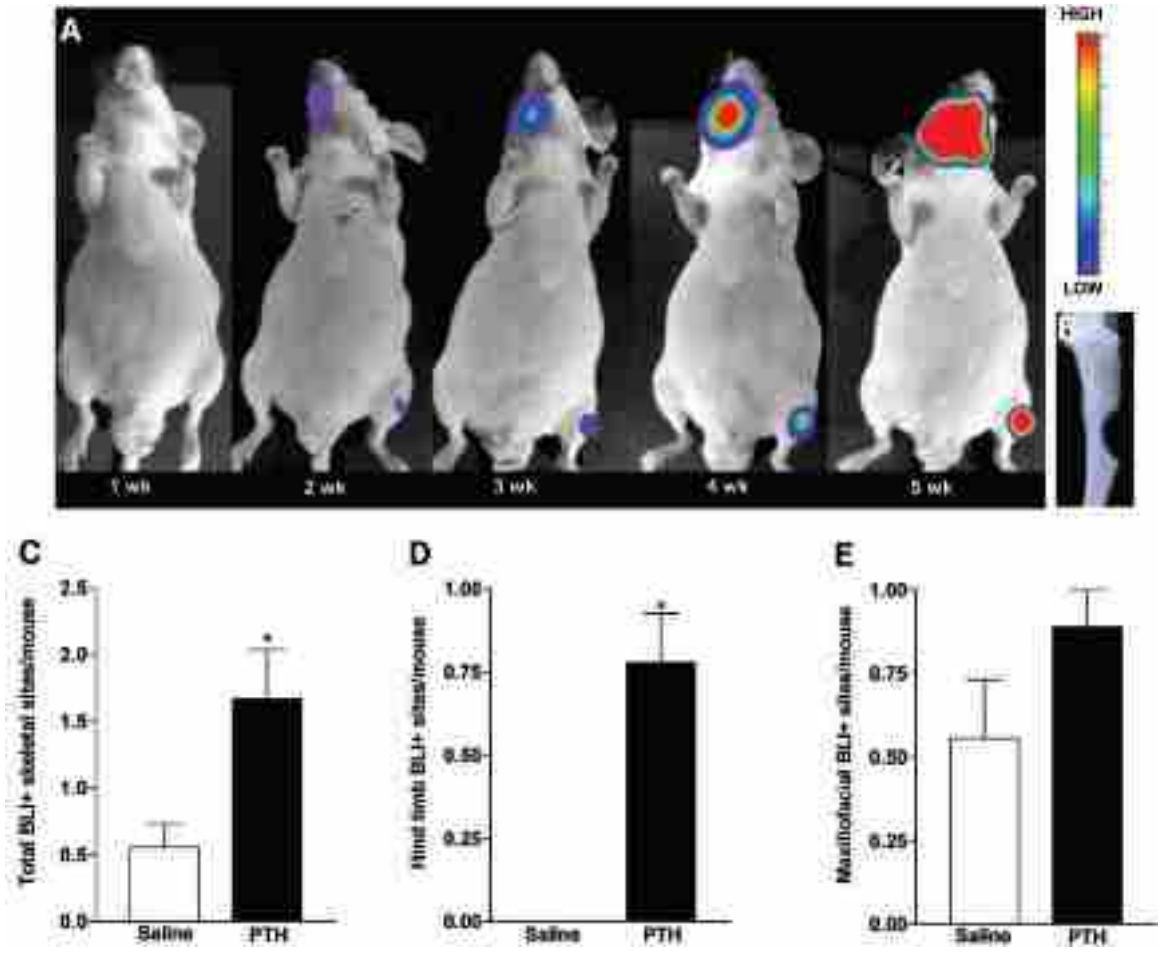

FIG. 3. PC-3^{Luc} cell localization in adult mice treated with rhPTH [1–34] or saline. A, Weekly progression of PC-3^{Luc} cell tumor growth in the craniofacial region and left hind limb of a representative PTH-treated mouse. B, Radiographically, the hind limb BLI signal correlated with a large osteolytic lesion affecting both the cortical and cancellous bone. C, The number of BLI metastatic foci in total skeletal sites (including both the hind limb and craniofacial BLI signals) in mice treated with PTH was significantly higher *vs.* saline-treated controls (*, $P < 0.02$). D, BLI signals in the hind limbs were present only in PTH-treated mice, whereas the craniofacial region (E) was affected in both groups. Here, more mean positive BLI signals per mouse were observed in the PTH group; however, no statistical significance was observed *vs.* the controls. Data represent the mean ± SEM, n = 9 mice per group.

sected 4 wk after the conclusion of PTH treatment. These data emphasize the nature of metastatic cell systems to increase bone resorption and bone formation often in a manner that is uncoupled and, in this case, the result being an unbalanced loss in bone mass.

Because of the considerable increase in BLI-positive signals in skeletal sites known to be especially responsive to PTH effects on bone turnover (*i.e.* distal femoral/proximal tibial metaphyses), in the third part of this study we evaluated PC-3^{Luc} cell localization after treatment with an osteoclastic bone resorption inhibitor under the systemic influence of PTH. ZA (3 μg/d), a third-generation aminobisphosphonate known for its potent osteoclast inhibitory effects (20), was administered sc in conjunction with rhPTH [1–34] (PTH/ZA group) after a similar approach as the previous two protocols (Fig. 1C). We found a statistically significant reduction in tumor localization in mean total skeletal sites in the PTH/ZA-treated mice (0.83 ± 0.21) when compared with mice injected with rhPTH [1–34] only (1.46 ± 0.22) (Fig. 5A). Specifically, a marked reduction in mean hind limb BLI-positive sites per mouse was observed after PTH/ZA treatment (0.17 ± 0.11) compared with PTH-treated mice (0.54 ± 0.14) (Fig. 5B). Although there was a lower incidence of BLI-positive sites in the craniofacial region of the PTH/ZA-treated mice, the difference was not statistically significant (Fig. 5C). In addition, no difference was found in the distribution of metastatic soft tissue lesions between groups (data not shown). Overall, these findings suggest that the use of a potent antiresorptive agent, such as ZA, in the presence of a high bone turnover state was effective in disrupting the bone remodeling process and preventing tumor cell localization in bone.

The bone turnover status was evaluated and confirmed by determining serum levels of bone turnover markers in a parallel group of adult mice treated with either saline, rhPTH [1–34], or PTH/ZA for 1 wk before the intracardiac inoculation of tumor cells. Mean serum osteocalcin, a bone formation marker, was significantly increased in rhPTH [1–34]-treated mice (419 ± 18.8 ng/ml) compared with mice treated with PTH/ZA (333.5 ± 20 ng/ml) or saline (298 ± 27.5

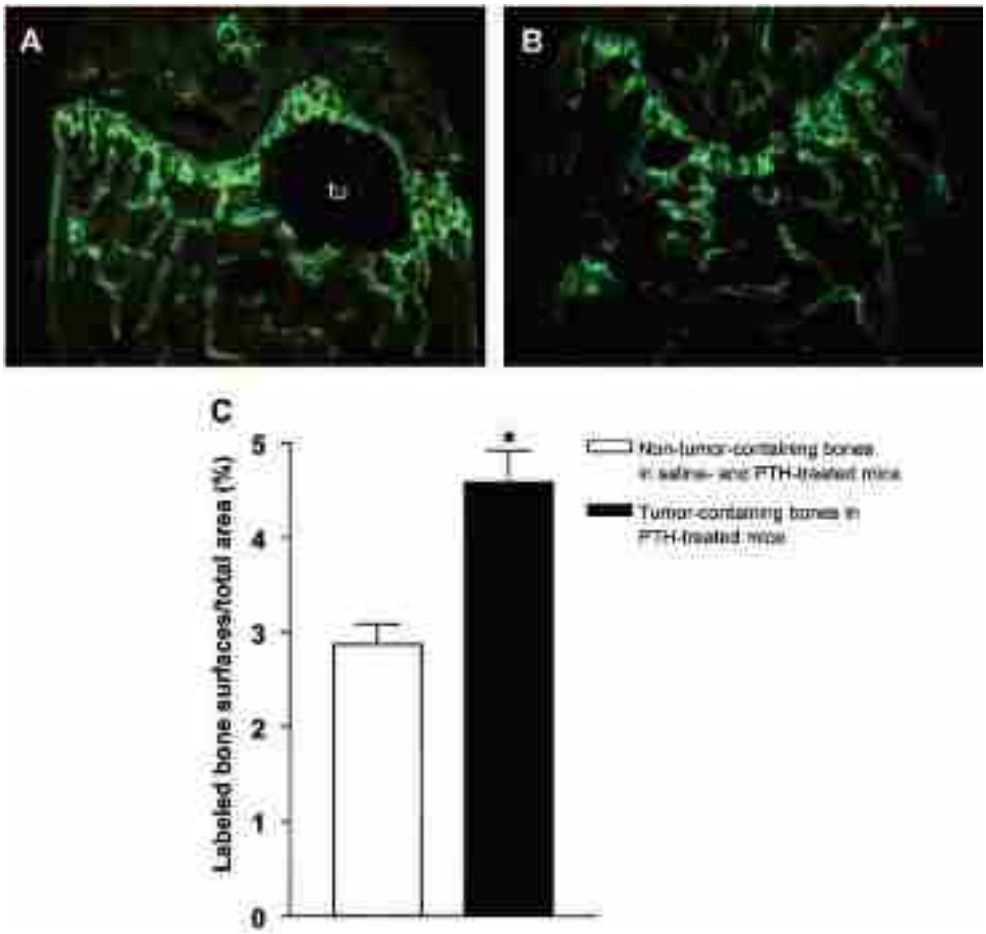

FIG. 4. Calcein uptake by mineralizing bone surfaces in tumor- and non-tumor-containing distal femoral metaphyses of rhPTH [1–34]- and saline-treated adult mice. At 5 wk after PC-3^{Luc} intracardiac inoculation, a marked increase in calcein uptake was observed in metaphyseal bone surfaces and in the trabeculae surrounding a tumor-associated lytic lesion (tu) in a representative PTH-treated mouse (A) *vs.* a tumor-free femur from a saline-treated mouse (B) (×100). C, Histomorphometric analysis revealed a significant increase in calcein-labeled bone surfaces per total area in PTH-treated mice (n = 4) compared with non-tumor containing femora from PTH- and saline-treated mice (n = 8) (*, $P < 0.01$). Data represent the mean ± SEM.

ng/ml) (Fig. 6A). The effect on osteoclastic activity was validated by the presence of a higher number of TRAP+ osteoclasts per millimeter of bone on the endosteal and trabecular surfaces of proximal tibial metaphyses in PTH-treated adult mice (10.2 ± 1.86) compared with the other two groups (PTH/ZA, 5.15 ± 0.52; saline, 3.6 ± 0.56) (Fig. 6B). These results were further confirmed by a significant increase in serum TRAP 5b levels in mice administered rhPTH [1–34] (3.13 ± 0.57 U/liter) *vs.* PTH/ZA (0.98 ± 0.10 U/liter) or saline (1.3 ± 0.18 U/liter) (Fig. 6C). In young mice, 1 wk of either saline or PTH treatment before PC-3^{Luc} cell inoculation resulted in serum TRAP 5b levels comparable to those observed in PTH-treated adult mice (saline, 2.88 ± 0.17 U/liter; PTH, 3.99 ± 0.18 U/liter) (Fig. 6D). These data support the impact of PTH on bone turnover in adult mice at the time when tumor cells were systemically delivered. Moreover, these findings suggest that, regardless of the treatment administered to young mice before tumor inoculation, the higher bone resorptive activity of a growing skeleton may have played an important role in facilitating a similar occurrence of tumor skeletal localization between PTH- and saline-treated mice.

Skeletal sites from adult mice that were administered rhPTH [1–34] for 1 wk before tumor inoculation also demonstrated a qualitative increase in bone marrow cell proliferation as evaluated by BrdU immunostaining (Fig. 6, E–G). These studies provide evidence that prostate cancer cell colonization occurs more frequently in skeletal sites rich in marrow cellularity under an active state of turnover. The significance of bone turnover in the formation of skeletal metastases was evident by the reduction in osteoclastic activity and tumor occurrence after treatment with ZA administered simultaneously with an effective stimulator of bone turnover such as PTH.

Discussion

Metastasis is the most common complication associated with the majority of deaths in patients suffering from cancer. The ability of metastatic cells to colonize, grow, and survive in secondary sites requires the completion of a series of highly complex, sequential, and interdependent biological events (31). Although these events are relatively common to most metastatic tumors, the final secondary organ destina-

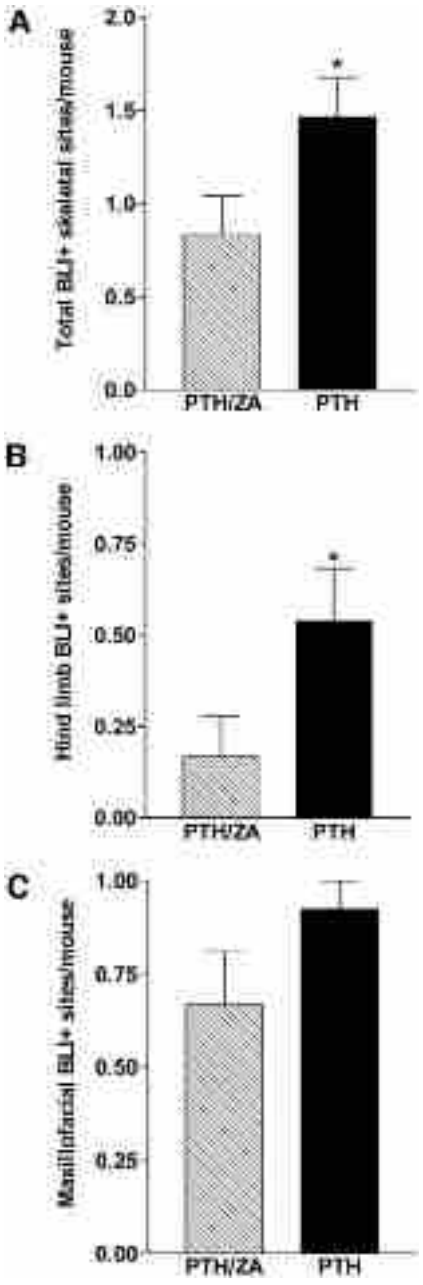

FIG. 5. PC-3^{Luc} cell localization in adult mice treated with rhPTH [1–34] only or in conjunction with ZA (PTH/ZA). A, The number of BLI metastatic foci in total skeletal sites (including both the hind limb and craniofacial BLI signals) in mice treated with PTH/ZA (n = 12) was significantly reduced when compared with PTH only-treated mice (n = 13) (*, $P < 0.05$). B, The reduction in BLI-positive signals was statistically significant in the hind limbs of mice treated with PTH/ZA (*, $P < 0.05$) but no difference in the distribution of metastatic foci affecting the craniofacial region was observed between groups (C). Data represent the mean ± SEM.

tion may vary among different types of cancer. Common cancers, such as those affecting the prostate and mammary glands, frequently demonstrate a particular predilection to disseminate and form metastases in the skeleton. Once in the bone microenvironment, the interaction between tumor-derived factors and bone cells results in the development of osteolytic, osteoblastic, or mixed lesions. However, it is still not clearly understood which skeletal-specific factors are among the critical determinants of the preferential localization of metastatic cells in bone. Because bone metastases are generally associated with critical and costly complications that include humoral hypercalcemia of malignancy, severe pain, spinal cord compression, and pathological fractures due to the increased fragility of abnormally immature bone (4, 5), validation of these factors may provide a better understanding of the pathophysiology of the disease, ultimately leading to the development of improved therapeutic interventions and patient survival rates.

Prostate cancer skeletal metastases are often found in areas containing increased marrow cellularity and active bone remodeling such as the axial skeleton and long bone metaphyses (7). These observations underscore the important role played by specific host factors in determining the nonrandom pattern of tumor localization in the skeleton, hence supporting the seed and soil hypothesis of cancer dissemination (6). However, whether increased bone turnover predisposes the skeleton to prostate cancer colonization is unknown. We recently reported that, after the intracardiac inoculation of PC-3^{Luc} cells, young immunodeficient mice developed more skeletal metastatic lesions, as determined by BLI, compared with older mice (18). These findings suggest that active skeletal growth and increased marrow cellularity, as occur in young mice, may be key microenvironmental host factors favoring the preferential localization of metastatic prostate cancer in bone.

In the present study, we confirmed this hypothesis by demonstrating in a similar experimental model that more PC-3^{Luc} metastatic foci were found in the skeleton of adult mice treated with the amino-terminal fragment of the calciotropic hormone PTH, a widely used and effective stimulator of bone turnover. In young mice, skeletal metastases formed in the hind limbs and craniofacial region equally between groups. However, in sexually mature adult mice, in which skeletal growth is at a more steady state, the influence of a high bone turnover condition stimulated by PTH treatment resulted in a 3-fold increase in BLI-positive total skeletal signals when compared with saline-treated controls. Studies using a similar PTH [1–34] dosing regimen for 2–7 wk in murine and other rodent model systems report increases in bone mass and markers of bone turnover including serum osteocalcin, serum and bone extract alkaline phosphatase (markers of bone formation), as well as TRAP (marker of bone resorption) (26, 27, 32). The results of the present study are in agreement with those findings because we observed that similar serum markers of bone turnover increased significantly in PTH-treated adult mice before tumor inoculation. We further validated these data by demonstrating an increased number of osteoclasts and marrow cell proliferation in the PTH group, substantiating our hypothesis that higher marrow cellular activity may serve as a potential factor to facilitate tumor skeletal colonization. Whereas rhPTH [1–34] in our studies was primarily used due to its potent activity as stimulator of bone turnover, recent epidemiological data have identified an association between hyperparathyroidism and the incidence of breast cancer. A record-linkage follow-up study in Sweden found that a prior occurrence of primary parathyroid adenoma was signifi-

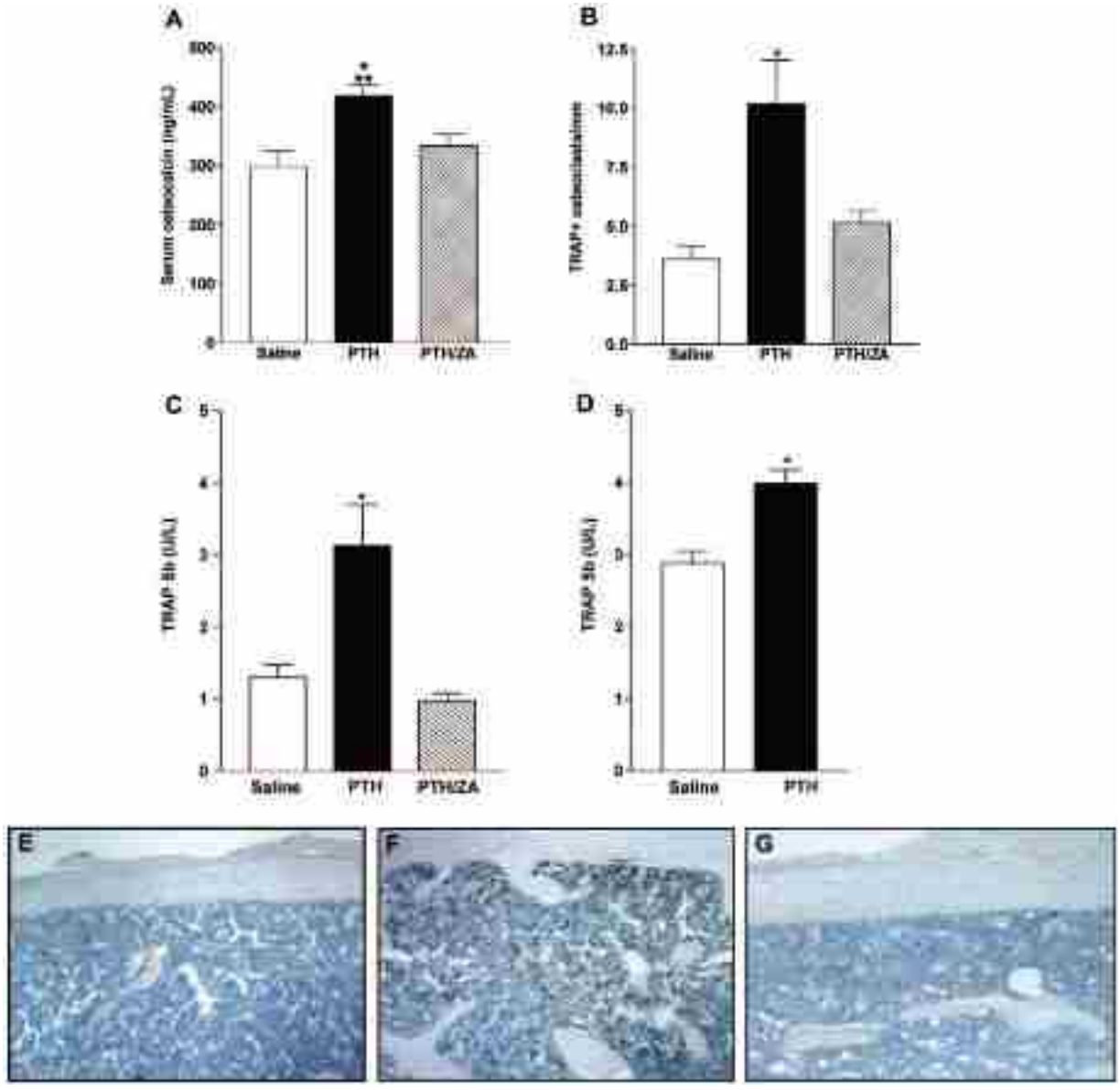

FIG. 6. Serum markers of bone turnover and marrow cell proliferation at the time of PC-3^{Luc} intracardiac inoculation (after 7 d of pharmacologic treatment). A subset of animals from each group was killed after 1 wk of pharmacological treatments to characterize changes occurring in bone turnover at the time of PC-3^{Luc} inoculation. A, Levels of serum osteocalcin, a bone formation marker, were significantly increased in rhPTH [1–34]-treated adult mice (n = 10) compared with mice treated with PTH/ZA (n = 6) (*, $P < 0.02$) or saline (n = 8) (**, $P < 0.002$). B, Osteoclastic activity was demonstrated by the presence of a higher mean number of TRAP+ osteoclasts per millimeter of bone on the endosteal and trabecular surfaces of proximal tibial metaphyses in PTH-treated adult mice compared with the other two groups (*, $P < 0.03$). C, Mean serum TRAP 5b, an osteoclast-specific bone resorption marker, was increased in mice administered with PTH *vs.* PTH/ZA or saline (*, $P < 0.02$). D, In young mice (n = 10/group), serum TRAP 5b levels were elevated with rhPTH [1–34] (*, $P < 0.001$ *vs.* saline) but were comparable to the levels observed in adult PTH-treated mice. BrdU immunostaining of representative proximal tibial metaphyses from mice that were administered PTH (F) demonstrated a qualitative increase in bone marrow cell proliferation compared with saline (E)- and PTH/ZA (G)-treated mice (×100). Data represent mean ± SEM.

cantly related to the risk of developing breast cancer (33). Based on the results of our studies, these findings are clinically relevant because they raise the possibility that increased bone turnover associated with hyperparathyroidism might predispose circulating cancer cells to preferentially colonize the skeleton. Although the authors did not evaluate the incidence of bone metastases in their patient cohort, additional studies should address this potential clinical complication.

We also found that when the bisphosphonate ZA, an inhibitor of bone resorption, was administered to adult mice in conjunction with rhPTH [1–34], a significant reduction in the number of BLI-positive total skeletal signals was observed. Similar to the saline-treated group, the PTH/ZA-treated animals did not show increased serum levels of bone turnover markers, number of osteoclasts, or marrow cell proliferation, most likely due to the disruption in the coupling process between osteoclastic bone resorption and osteoblastic bone

formation (34). Due to their unique chemical composition, bisphosphonates have strong affinity for bone and show preferential incorporation into osteoclastic cells, resulting in the selective inhibition of bone resorption through osteoclast apoptosis (35). Our data suggest that ZA effectively prevented tumor localization in the hind limb region even under the impact of a potent inducer of bone cellular activity such as PTH. Consistent with our results, a study in orchidectomized athymic mice showed that androgen ablation after surgical castration resulted in increased bone resorption and facilitated the development of PC-3 skeletal metastases (36). A decrease in the occurrence of PC-3 bone metastases was observed when ZA was administered from the time of the surgery, 4 wk before tumor inoculation. The authors concluded that bone resorption inhibitors, such as bisphosphonates, could benefit hypogonadal men with advanced prostate cancer by decreasing bone metastases as well as preventing bone resorption. The inhibitory effect of this drug on skeletal tumor localization may be associated with cellular and biochemical alterations in the bone microenvironment that act to deprive circulating tumor cells of chemotactic, adhesive, and/or growth-promoting cues (37). Recent studies also point to the direct beneficial actions of ZA as an antitumor agent by demonstrating inhibition of prostate cancer cell proliferation and invasion, and promotion of apoptosis *in vitro* and *in vivo* (38, 39). In fact, ZA was found to reduce prostate cancer tumor growth in the skeleton but not in tumors developed in an extraskeletal location (39). These findings suggest that the selective inhibition of tumor growth in bone is particularly associated with the specific affinity of this type of drug to skeletal tissue. Surprisingly, we did not observe such an effect in the craniofacial area. The anatomical disparity in the distribution of skeletal metastases between the hind limb *vs.* craniofacial regions was a consistent finding. Craniofacial metastatic foci, particularly affecting the mandibular region, were present in most animals regardless of treatment. In general, oral and craniofacial metastases from prostate cancer and other primary tumors are extremely rare in humans, comprising less than 1% of all cancers affecting this region. However, when they occur, the posterior mandible is more commonly involved (40, 41). We suspect that the increased occurrence of craniofacial tumor foci in this study may be associated with inherent biological characteristics of the murine model. It is possible that the unique pattern of continuous eruption of mandibular incisors provides cellular activity consistent with high turnover in a native niche, thus facilitating tumor localization and growth (42). If this is true it also substantiates our original hypothesis.

We also observed a higher incidence of metastases affecting specifically the hind limbs in the PTH-treated group. This phenomenon is likely related to the higher responsiveness to PTH in the distal femoral/proximal tibial region compared with other skeletal sites, which generally leads to increases in bone mass and bone turnover markers (43). It is also of interest that the influence of PTH on the bone/bone marrow microenvironment has been recently explored *in vivo*. Transgenic mice producing osteoblast-specific, activated PTH/PTHrP receptors demonstrate an increase in the number of osteoblastic cells supporting hematopoietic stem cell proliferation via the Jag1/Notch axis (44). In addition, after a PTH dosing regimen similar to the one used in our study, the bone marrow of wild-type mice also had an increased number of osteoblastic cells and hematopoietic stem cells. Interestingly, these *in vivo* data were analyzed in proximal tibial metaphyses, the area in which we observed more metastatic lesions in the hind limbs. Consistent with these observations, we have also found through *in vitro* and in *vivo* approaches that PTH increases the secretion of osteoblast-derived stromal-derived factor-1, a major chemokine known for its powerful chemoattraction of mature and early hematopoietic cells as well as metastatic prostate cancer cells expressing its receptor CXCR4 (Ref. 9 and Jung, Y., J. Wang, A. Schneider, Y. Sun, A. J. Koh-Paige, N. I. Osman, L. K. McCauley, and R. S. Taichman, submitted for publication). For the purpose of our study, these results emphasize a novel regulatory action of PTH in bone/bone marrow cellular interactions and its potential role in promoting homing and localization of normal and tumor cells in bone. Therefore, it is likely that the PTH-induced pharmacological modulation of bone turnover in our bone metastasis model system involves some of these molecular events. In summary, our findings provide new evidence for the role of a fertile host microenvironment to promote cancer cell skeletal localization. We demonstrate that increased bone turnover and marrow cell proliferation in response to a calciotropic hormone leads to the preferential dissemination of prostate cancer to the skeleton. Additional investigations should address in greater detail the cellular and molecular basis of this phenomenon. In addition, early monitoring of bone turnover markers and pharmacological strategies to limit bone remodeling when elevated should be experimentally evaluated as a preventive measure in cancer patients at risk of developing skeletal metastases.

Acknowledgments

We thank Dr. Russell Taichman for helpful discussions during the course of this study; Daniel Hall (University of Michigan Center for Molecular Imaging), Chris Strayhorn (University of Michigan, School of Dentistry Histology Core Facility), and Joanne Schoonmaker (State University of New York Upstate Medical University) for technical assistance with bioluminescent optical imaging and histological preparation of samples; and Janice Berry for useful comments in the preparation of the manuscript.

Received September 13, 2004. Accepted December 23, 2004.

Address all correspondence and requests for reprints to: Dr. Laurie K. McCauley, Department of Periodontics/Prevention/Geriatrics, School of Dentistry, Room 3343, University of Michigan, 1011 North University Avenue, Ann Arbor, Michigan 48109-1078. E-mail: mccauley@umich.edu.

This work was supported by National Cancer Institute Specialized Program of Research Excellence in Prostate Cancer Grant 1-P50-CA69569 and National Cancer Institute Grant1-P01-CA093900.

References

1. **Jemal A, Tiwari RC, Murray T, Ghafoor A, Samuels A, Ward E, Feuer EJ, Thun MJ; American Cancer Society** 2004 Cancer statistics, 2004. CA Cancer J Clin 54:8–29
2. **Nelson WG, De Marzo AM, Isaacs WB** 2003 Prostate cancer. N Engl J Med 349:366–381
3. **Rubin MA, Putzi M, Mucci N, Smith DC, Wojno K, Korenchuk S, Pienta KJ** 2000 Rapid ("warm") autopsy study for procurement of metastatic prostate cancer. Clin Cancer Res 6:1038–1045
4. **Mundy GR** 2002 Metastasis to bone: causes, consequences and therapeutic opportunities. Nat Rev Cancer 2:584–593

5. **Roodman GD** 2004 Mechanisms of bone metastasis. N Engl J Med 350:1655–1664
6. **Paget S** 1889 The distribution of secondary growths in cancer of the bones. Lancet 1:571–573
7. **Imbriaco M, Larson SM, Yeung HW, Mawlawi OR, Erdi Y, Venkatraman ES, Scher HI** 1998 A new parameter for measuring metastatic bone involvement by prostate cancer: the Bone Scan Index. Clin Cancer Res 4:1765–1772
8. **Koeneman KS, Yeung F, Chung LWK** 1999 Osteomimetic properties of prostate cancer cells: a hypothesis supporting the predilection of prostate cancer metastasis and growth in the bone microenvironment. Prostate 39:246–261
9. **Taichman RS, Cooper C, Keller ET, Pienta KJ, Taichman NS, McCauley LK** 2002 Use of the stromal cell-derived factor-1/CXCR4 pathway in prostate cancer metastasis to bone. Cancer Res 62:1832–1837
10. **Sasaki A, Boyce BF, Story B, Wright KR, Chapman M, Boyce R, Mundy GR, Yoneda T** 1995 Bisphosphonate risedronate reduces metastatic human breast cancer burden in bone in nude mice. Cancer Res 55:3551–3557
11. **Michigami T, Hiraga T, Williams P, Niewolna M, Nishimura R, Mundy GR, Yoneda T** 2002 The effect of the bisphosphonate ibandronate on breast cancer metastasis to visceral organs. Breast Cancer Res Treat 75:249–258
12. **Saad F, Gleason DM, Murray R, Tchekmedyian S, Venner P, Lacombe L, Chin JL, Vinholes JJ, Goas JA, Zheng M** 2004 Long-term efficacy of zoledronic acid for the prevention of skeletal complications in patients with metastatic hormone-refractory prostate cancer. J Natl Cancer Inst 96:878–882
13. **Kostenuik PJ, Orr FW, Suyama K, Singh G** 1993 Increased growth rate and tumor burden of spontaneously metastatic Walker 256 cancer cells in the skeleton of bisphosphonate-treated rats. Cancer Res 15:5452–5457
14. **Guise TA, Yin JJ, Taylor SD, Kumagai Y, Dallas M, Boyce BF, Yoneda T, Mundy GR** 1996 Evidence for a causal role of parathyroid hormone-related protein in the pathogenesis of human breast cancer-mediated osteolysis. J Clin Invest 98:1544–1549
15. **Edinger M, Sweeney TJ, Tucker AA, Olomu AB, Negrin RS, Contag CH** 1999 Noninvasive assessment of tumor cell proliferation in animal models. Neoplasia 1:303–310
16. **Rehemtulla A, Stegman LD, Cardozo SJ, Gupta S, Hall DE, Contag CH, Ross BD** 2000 Rapid and quantitative assessment of cancer treatment response using in vivo bioluminescence imaging. Neoplasia 2:491–495
17. **Rosol TJ, Tannehill-Gregg SH, Corn S, Schneider A, McCauley LK** 2004 Animal models of bone metastasis. Cancer Treat Res 118:47–81
18. **Kalikin LM, Schneider A, Thakur MA, Fridman Y, Griffin LB, Dunn RL, Rosol TJ, Shah RB, Rehemtulla A, McCauley LK, Pienta KJ** 2003 In vivo visualization of metastatic prostate cancer and quantitation of disease progression in immunocompromised mice. Cancer Biol Ther 2:656–660
19. **Hock JM, Fitzpatrick LA, Bilezikian JP** 2002 Actions of parathyroid hormone. In: Bilezikian JP, Raisz LG, Rodan GA, eds. Principles of bone biology. San Diego: Academic Press; 463–482
20. **Green JR, Clezardin P** 2002 Mechanisms of bisphosphonate effects on osteoclasts, tumor cell growth, and metastasis. Am J Clin Oncol 25:S3–S9
21. **Nyati MK, Symon Z, Kievit E, Dornfeld KJ, Rynkiewicz SD, Ross BD, Rehemtulla A, Lawrence TS** 2002 The potential of 5-fluorocytosine/cytosine deaminase enzyme prodrug gene therapy in an intrahepatic colon cancer model. Gene Ther 9:844–849
22. **Schneider A, Taboas J, McCauley LK, Krebsbach PH** 2003 Skeletal homeostasis in tissue-engineered bone. J Orthop Res 21:859–864
23. **McCauley LK, Rosol TJ, Capen CC, Horton JE** 1989 A comparison of bone turnover in athymic (nude) and euthymic mice: biochemical, histomorphometric, bone ash and in vitro studies. Bone 10:29–34
24. **Erben RG** 1997 Embedding of bone samples in methylmethacrylate: an improved method suitable for bone histomorphometry, histochemistry, and immunohistochemistry. J Histochem Cytochem 45:307–313
25. **Ling Q, Raggatt LJ, Partridge NC** 2004 Parathyroid hormone: a double-edged sword for bone metabolism. Trends Endocrinol Metab 15:60–65
26. **Mohan S, Kutilek S, Zhang C, Shen HG, Kodma Y, Srivastava AK, Wergedal JE, Beamer WG, Baylink DJ** 2000 Comparison of bone formation responses to parathyroid hormone (1–34), (1–31) and (2–34) in mice. Bone 27:471–478
27. **Frolick CA, Black EC, Cain RL, Satterwhite JH, Brown-Augsburger PL, Sato M, Hock JM** 2003 Anabolic and catabolic bone effects of human parathyroid hormone (1–34) are predicted by duration of hormone exposure. Bone 33:372–379
28. **Corey E, Quinn JE, Bladou F, Brown LG, Roudier MP, Brown JM, Buhler KR, Vessella RL** 2002 Establishment and characterization of osseous prostate cancer models: intra-tibial injection of human prostate cancer cells. Prostate 52:20–23
29. **Stewart AF, Vignery A, Silverglate A, Ravin ND, LiVolsi V, Broadus AE, Baron R** 1982 Quantitative bone histomorphometry in humoral hypercalcemia of malignancy: uncoupling of bone cell activity. J Clin Endocrinol Metab 55:219–227
30. **Guise TA, Mohammad KS** 2004 Endothelins in bone cancer metastases. Cancer Treat Res 118:197–212
31. **Fidler IJ** 2002 The pathogenesis of cancer metastasis: the "seed and soil" hypothesis revisited. Nat Rev Cancer 3:1–6
32. **Hock JM, Gera I, Fonseca J, Raisz LG** 1988 Human parathyroid hormone-(1–34) increases bone mass in ovariectomized and orchidectomized rats. Endocrinology 122:2899–2904
33. **Michels KB, Xue F, Brandt L, Ekbom A** 2004 Hyperparathyroidism and subsequent incidence of breast cancer. Int J Cancer 110:449–451
34. **Manolagas SC** 2000 Birth and death of bone cells: basic regulatory mechanisms and implications for the pathogenesis and treatment of osteoporosis. Endocr Rev 21:115–137
35. **Yoneda T, Hashimoto N, Hiraga T** 2004 Bisphosphonate actions on bone and visceral metastases. Cancer Treat Res 118:213–229
36. **Padalecki SS, Carreon M, Grubbs B, Cui Y, Guise TA** 2003 Androgen deprivation enhances bone loss and prostate cancer metastases to bone: prevention by zoledronic acid. Oncology 17:32 (Abstract)
37. **Croucher P, Jagdev S, Coleman R** 2003 The anti-tumor potential of zoledronic acid. Breast 2(Suppl 2):S30–S36
38. **Lee MV, Fong EM, Singer FR, Guenette RS** 2001 Bisphosphonate treatment inhibits the growth of prostate cancer cells. Cancer Res 61:2602–2608
39. **Corey E, Brown LG, Quinn JE, Poot M, Roudier MP, Higano CS, Vessella RL** 2003 Zoledronic acid exhibits inhibitory effects on osteoblastic and osteolytic metastases of prostate cancer. Clin Cancer Res 9:295–306
40. **Hirshberg A, Leibovich P, Buchner A** 1994 Metastatic tumors to the jawbones: analysis of 390 cases. J Oral Pathol Med 23:337–341
41. **van der Waal RIF, Buter J, van der Waal I** 2003 Oral metastases: report of 24 cases. Br J Oral Maxillofac Surg 41:3–6
42. **Tiffee JC, Xing L, Nilsson S, Boyce BF** 1999 Dental abnormalities associated with failure of tooth eruption in *src* knockout and *op/op* mice. Calcif Tissue Int 65:53–58
43. **Iida-Klein A, Zhou H, Lu SS, Levine LR, Ducayen-Knowles M, Dempster DW, Nieves J, Lindsay R** 2002 Anabolic action of parathyroid hormone is skeletal site specific at the tissue and cellular levels in mice. J Bone Miner Res 17:808–816
44. **Calvi LM, Adams GB, Welbrecht KW, Weber JM, Olson DP, Knight MC, Martin RP, Schipani E, Divieti P, Bringhurst FR, Milner LA, Kronenberg HM, Scadden DT** 2003 Osteoblastic cells regulate the haematopoietic stem cell niche. Nature 425:841–846

***Endocrinology* is published monthly by The Endocrine Society (http://www.endo-society.org), the foremost professional society serving the endocrine community.**